

Renormalization in Coulomb gauge QCD

A. Andraši *

'Rudjer Bošković' Institute, Zagreb, Croatia

John C. Taylor[†]

*Department of Applied Mathematics and Theoretical Physics,
University of Cambridge, UK*

27 Oct. 2010

Abstract

In the Coulomb gauge of QCD, the Hamiltonian contains a non-linear Christ-Lee term, which may alternatively be derived from a careful treatment of ambiguous Feynman integrals at 2-loop order. We investigate how and if UV divergences from higher order graphs can be consistently absorbed by renormalization of the Christ-Lee term. We find that they cannot.

Pacs numbers: 11.15.Bt; 11.10.Gh

Keywords: Coulomb gauge; Renormalization; QCD

*aandrasi@rudjer.irb.hr

†J.C.Taylor@damtp.cam.ac.uk

1 Introduction

The Coulomb gauge in QCD has some attractive properties. It is the only gauge which is explicitly unitary, all the state vectors being physical (with transverse gluons) with positive norm. (Axial gauges suffer from ambiguous denominators $1/n.k$ in Feynman propagators.) The Coulomb gauge has been used in lattice simulations, see for instance[1].

Nevertheless, the Coulomb gauge is not straightforward. First, in individual Feynman diagrams, even at 1-loop order, there are linear “energy divergences” of the form

$$\int dk_0 F \tag{1}$$

where F is independent of k_0 . This problem is cured by going to the Hamiltonian, phase-space, formalism, in which the conjugate field E_i^a to A_i^a is introduced. Even then, introducing quark loops brings back energy divergences in individual graphs which must be cancelled by combining graphs [2].

In the Hamiltonian formalism, at 1-loop level, there are formally divergent integrals of the form (we use P for the spacial part of the 4-vector p)

$$\int dp_0 \frac{p_0}{p_0^2 - P^2} F \tag{2}$$

where again F is independent of p_0 . It is natural to take (2) to be zero. This can be justified by taking the Coulomb gauge to be the limit, when a certain parameter tends to zero, of a gauge interpolating between the Feynman gauge and the Coulomb gauge [5] [6].

To 2-loop order there are more subtle difficulties, in the appearance of non-convergent integrals of the form

$$\int dp_0 dq_0 \frac{p_0}{p_0^2 - P^2} \frac{q_0}{q_0^2 - Q^2} F(P, Q, \dots) \tag{3}$$

(where a Feynman $i\eta$ is understood in the denominators). It has been shown [4] [6] that these divergences are resolved when suitable sets of graphs are added. This is achieved partly by the use of the identity

$$\int dp_0 dq_0 dr_0 \delta(p_0 + q_0 + r_0) \left[\frac{p_0}{p_0^2 - P^2} \frac{q_0}{q_0^2 - Q^2} + \frac{q_0}{q_0^2 - Q^2} \frac{r_0}{r_0^2 - R^2} + \frac{r_0}{r_0^2 - R^2} \frac{p_0}{p_0^2 - P^2} \right] = -\pi^2 \tag{4}$$

though again an interpolating gauge is necessary for a complete rigorous treatment. We shall call graphs which contain the integral (3) *A-graphs* (A for “ambiguous”) and non-convergent integrals like (3) *A-integrals*. Another rule about the *A-integrals* is that integrals like the square of (2), that is of the form

$$\int dp_0 \frac{p_0}{p_0^2 - P^2} F(P) \int dq_0 \frac{q_0}{q_0^2 - Q^2} G(Q) \tag{5}$$

are zero. This is consistent with (2), but the rule can again be justified rigorously [6] by using an interpolating gauge. We call this rule "factorization".

Previous to this work, an equivalent result has been derived by Christ and Lee [7]. They noted an operator ordering ambiguity in the non-local Coulomb interaction in the Coulomb gauge Hamiltonian. They resolved this by the addition of extra operators to the Hamiltonian, at the same time defining the Feynman integration so that integrals like (3) are zero. (Though this definition must be used with caution in view of the identity (4).)

All the above work is concerned with the energy integrals, with the spatial momenta temporarily held fixed. When this is done, it has been shown [4] [6] that non-convergent *A-integrals* appear at 2-loop order only, not at 1-loop and not at 3-loop and higher. Problems might arise when the above energy divergences are considered along with ordinary UV divergences and the necessity of renormalization [6] [8]. The standard method of renormalization demands that UV divergent sub-graphs are computed and renormalized before insertion in the main graph. This order of integration might conflict with the use of (4), which requires two energy integrals to be done before either of the corresponding integrals over spatial momenta. However, consider the sub-graphs of an *A-graph*. Such a sub-graph contains (2) and so is zero. Therefore there is no UV divergence in the sub-graph and no renormalization is needed. This is consistent, since a Feynman integral of the form (with dimensional regularization)

$$\int d^{3-\epsilon} P d q_0 d p_0 \frac{p_0}{p^2 - P^2} \frac{q_0}{q_0^2 - Q^2} H(P, Q) \quad (6)$$

never has a pole $\frac{1}{\epsilon}$, where $\epsilon = 4 - n$ and n is the number of space-time dimensions.

In this paper, we study another such possible conflict: the insertion of UV divergent sub-graphs into *A-graphs*. For simplicity, we choose the sub-graphs to be quark loops (which would dominate for large N_f , the number of families). We are not permitted to perform all three energy integrals first, with all spatial momenta held fixed: renormalization demands that we do all the integrals, energy and spatial, in the UV divergent sub-graph first. Thus we are concerned with integrals of the form

$$\int d p_0 d q_0 d s_0 d^{3-\epsilon} S J(p_0, q_0, P, Q; s_0, S) \quad (7)$$

where the q -integration is an UV divergent sub-graph (a fermion loop). We hold P and Q fixed, but we have to do both the s_0 and the S integrations first because a renormalization subtraction must be made before doing other integrals. So we require the high-energy behaviour of the subgraphs (2, 3, and 4-gluon diagrams) in order to study the convergence of the remaining two energy integrals. We can obtain this high-energy behaviour from the Ward identities obeyed by the quark loops which determine all the high energy behaviours in terms of one function, the gluon self-energy $S(p)$. When an attempt is made to use the identity (4), this function S appears in various places. The question is whether these extra insertions spoil the identity. We find that they do. We

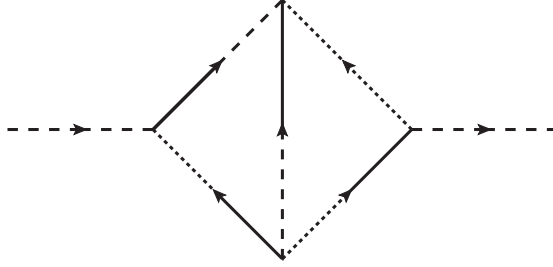


Figure 1: The example of the 2-loop graphs, graph 1B. Continuous lines represent \mathbf{E} , dashed lines \mathbf{A} and dotted lines \mathbf{A}_0 .

conclude that the attempt to combine UV renormalization with the control of energy divergences leads to trouble.

Another way to regard this problem is to ask what are the fields and coupling constants in the Christ-Lee operator. Are they bare or renormalized quantities? Since Christ and Lee derived this from consideration of operation ordering of the original Hamiltonian, it seems they must be bare quantities. Then the question is how to re-express the operator in terms of useful, renormalized quantities.

In section 3, we derive the high-energy behaviour of the quark sub-graph loops by using the Ward identities, in section 4 we give the results for individual graphs and in section 5 there are conclusions.

2 Notation and graphs

We use the same notation and graphical conventions as in [3]. As well as lines for Coulomb interactions and for transverse gluon propagators, there are lines corresponding to transitions to E_i^a .

The relevant 2-loop graphs contain exactly two transverse propagators together with three Coulomb lines. They contain no vertex where three transverse gluons meet.

3 The high-energy limit of the quark loops

Let t^a be the colour matrices in the quark representation, with

$$\text{tr}(t^a t^b) = C_q \delta^{ab}. \quad (8)$$

The gluon self-energy from the quark loop is

$$\text{tr}(t^a t^b) S_{\mu_1 \mu_2}(p) = g^2 C_q \delta^{ab} (p_{\mu_1} p_{\mu_2} - p^2 \delta_{\mu_1 \mu_2}) S(p^2), \quad (9)$$

where

$$S(p^2) = 8i\pi^{2-\frac{\epsilon}{2}} \Gamma\left(\frac{\epsilon}{2}\right) \frac{\Gamma^2(2-\frac{\epsilon}{2})}{\Gamma(4-\epsilon)} [(-p^2 - i\eta)^{-\frac{\epsilon}{2}} - (\mu^2)^{-\frac{\epsilon}{2}}], \quad (10)$$

where a renormalization subtraction at a mass μ has been made.

The quark triangle is

$$\text{tr}(t^a [t^b, t^c]) V_{\mu_1 \mu_2 \mu_3}(p_1, p_2, p_3) \delta(p_1 + p_2 + p_3) \quad (11)$$

where V is totally anti-symmetric under permutations of 1, 2, 3.

The quark square is

$$\text{tr}(t^a t^b t^c t^d + t^d t^c t^b t^a) W_{\mu_1 \mu_2 \mu_3 \mu_4}(p_1, p_2, p_3, p_4) \delta(p_1 + p_2 + p_3 + p_4), \quad (12)$$

where W has cyclic symmetry in 1, 2, 3, 4 and symmetry under 1, 2, 3, 4 \rightarrow 4, 3, 2, 1. Because of these symmetries, there are in general three independent tensors W . But in the present case, the high-energy limits of the W 's are independent of the quark representation (apart from the overall factor C_q), and as a consequence there is an additional relation

$$W_{\mu_1 \mu_2 \mu_3 \mu_4} W(k_1, k_2, k_3, k_4) + (1, 2, 3 \rightarrow 3, 1, 2) + (1, 2, 3 \rightarrow 2, 3, 1) = 0. \quad (13)$$

The Ward identities connecting the quark loops are

$$k_{30} V_{000} - K_{3i} V_{00i} = S_{00}(k_1) - S_{00}(k_2) = K_1^2 S(k_1) - K_2^2 S(k_2), \quad (14)$$

$$k_{20} V_{00i} - K_{2j} V_{0ji} = S_{0i}(k_3) - S_{0i}(k_1) = k_{30} K_{3i} S(k_3) - k_{10} K_{1i} S(k_1), \quad (15)$$

$$k_{10} V_{0ij} - K_{1l} V_{lij} = S_{ij}(k_2) - S_{ij}(k_3) = \delta_{ij} [k_{20}^2 S(k_2) - k_{30}^2 S(k_3)], \quad (16)$$

$$k_{10} W_{00kl} - K_{1i} W_{i0kl} = V_{0kl}(k_1 + k_2, k_3, k_4) - V_{0kl}(k_1, k_2, k_3 + k_4), \quad (17)$$

$$\begin{aligned} k_{10} W_{0i0l}(k_1, k_2, k_3, k_4) - K_{1m} W_{mi0l}(k_1, k_2, k_3, k_4) \\ = V_{i0l}(k_1 + k_2, k_3, k_4) - V_{i0l}(k_2, k_3, k_1 + k_4). \end{aligned} \quad (18)$$

These may be solved in the limit where the time components of the momenta are much larger than the space components, to give

$$V_{0ij}(k_1, k_2, k_3) \approx k_{10}^{-1} \delta_{ij} [k_{20}^2 S(k_2) - k_{30}^2 S(k_3)], \quad (19)$$

$$V_{00i}(k_1, k_2, k_3) \approx \frac{K_{2i}}{k_{10}} [k_{20} S(k_2) + k_{30} S(k_3)] - \frac{K_{1i}}{k_{20}} [k_{30} S(k_3) + k_{10} S(k_1)], \quad (20)$$

$$\begin{aligned} V_{000}(k_1, k_2, k_3) \approx & -\frac{K_2 \cdot K_3}{k_{10}} [S(k_2) - S(k_3)] - \frac{K_3 \cdot K_1}{k_{20}} [S(k_3) - S(k_1)] \\ & - \frac{K_1 \cdot K_2}{k_{30}} [S(k_1) - S(k_2)]. \end{aligned} \quad (21)$$

We use notation $k_{12} = k_1 + k_2$ etc,

$$W_{00ml}(k_1, k_2, k_3, k_4) \approx -\delta_{ml} \left[\frac{k_{30}^2 S(k_3)}{k_{20} k_{120}} + \frac{k_{40}^2 S(k_4)}{k_{10} k_{120}} - \frac{k_{140}^2 S(k_1 + k_4)}{k_{10} k_{20}} \right], \quad (22)$$

$$W_{0i0l}(k_1, k_2, k_3, k_4) \approx \frac{1}{k_{10}k_{30}} \delta_{il} [k_{40}^2 S(k_4) + k_{20}^2 S(k_2) - (k_1 + k_2)_0^2 S(k_1 + k_2) - (k_1 + k_4)_0^2 S(k_1 + k_4)], \quad (23)$$

$$W_{000i}(k_1, k_2, k_3, k_4) \approx \frac{K_{2i}}{k_{10}k_{30}} [k_{340} S(k_3 + k_4) + k_{140} S(k_1 + k_4) + k_{20} S(k_2) - k_{40} S(k_4)] \\ + K_{1i} \left[-\frac{k_{340}}{k_{20}k_{30}} S(k_3 + k_4) - \frac{k_{10}}{k_{20}k_{230}} S(k_1) + \frac{k_{40}}{k_{30}k_{230}} S(k_4) \right] \\ + K_{3i} \left[-\frac{k_{140}}{k_{20}k_{10}} S(k_1 + k_4) - \frac{k_{30}}{k_{20}k_{120}} S(k_3) + \frac{k_{40}}{k_{10}k_{120}} S(k_4) \right], \quad (24)$$

$$W_{0000}(k_1, k_2, k_3, k_4) \approx \frac{K_1 \cdot K_3}{k_{20}k_{40}} [S(k_2 + k_3) + S(k_3 + k_4) - S(k_1) - S(k_3)] \\ - \frac{K_2 \cdot K_4}{k_{10}k_{30}} [S(k_1 + k_4) + S(k_3 + k_4) - S(k_2) - S(k_4)] \\ + (K_1 \cdot K_2) \left[\frac{S(k_1)}{k_{40}k_{340}} + \frac{S(k_2)}{k_{30}k_{340}} - \frac{S(k_1 + k_4)}{k_{30}k_{40}} \right] \\ + (K_3 \cdot K_4) \left[\frac{S(k_3)}{k_{20}k_{120}} + \frac{S(k_4)}{k_{10}k_{120}} - \frac{S(k_1 + k_4)}{k_{10}k_{20}} \right] \\ + (K_2 \cdot K_3) \left[\frac{S(k_3)}{k_{40}k_{140}} + \frac{S(k_2)}{k_{10}k_{140}} - \frac{S(k_3 + k_4)}{k_{40}k_{10}} \right] \\ + (K_4 \cdot K_1) \left[\frac{S(k_4)}{k_{30}k_{230}} + \frac{S(k_1)}{k_{20}k_{230}} - \frac{S(k_1 + k_2)}{k_{20}k_{30}} \right]. \quad (25)$$

The other components of V and W are negligible in this limit. Note that all the equations above apply only to the region where all the time components are much larger than any space component. So these equations are useful for checking convergence but not for finding the actual values of integrals. All subsequent equations are to be understood in the same way.

4 The gluon graphs with quark insertions

To take the simplest case, we look at graphs with just two external transverse gluon lines, with momenta k (in the Coulomb gauge, both real and virtual gluons are transverse).

We wish to test whether the ambiguous integrals like (2) combine into the unambiguous combinations (3) when quark loops insertions are present. We expect this to happen with the spatial parts of the gluon momenta held fixed, and it should therefore happen as an identity in the spatial momenta. With the basic set of independent invariant functions of P, Q, K ,

$$K^2, \quad P^2, \quad Q^2, \quad P'^2 = (P-K)^2, \quad Q'^2 = (Q-K)^2, \quad R'^2 = (K-P-Q)^2 \quad (26)$$

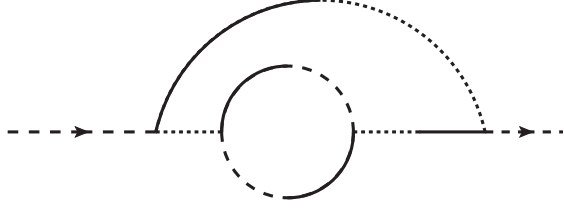


Figure 2: The example of the other class of diagrams which cannot contribute to the invariant in (27).

we choose an algebraically independent set of functions of these spatial momenta. We have the following classes of invariant functions

$$(a) \quad \frac{K^2}{P^2 P'^2 Q^2 Q'^2} \quad (27)$$

etc., i.e. with K^2 in the numerator and 4 different denominators (there are 5 such functions),

$$(b) \quad \frac{1}{P^2 Q^2 R'^2} \quad (28)$$

etc. with 3 denominators (there are 10 such functions),

$$(c) \quad \frac{P^2}{Q^2 Q'^2 P'^2 R'^2} \quad (29)$$

etc., that is one numerator (not K^2) and 4 other denominators (there are 5 such functions). Out of these 20 independent functions, we choose (27) in order to make the test. The functions in (a), (b) and (c) are sufficient for the graphs in fig.3 till fig.26. There is another class of diagrams, containing an internal self-energy part, of which one example is shown in fig.2. No graph of this second type can contribute to the invariant in (27), no matter how the variables P and Q are defined; so we need not consider any graph of this type.

The relevant graphs which contribute to K^2 are shown in fig.3 till fig.26. We use the notation

$$\alpha_{ab} = \frac{1}{4} g^6 (2\pi)^{-8} C_q^2 T(R) \delta_{ab} K^2 \int d^4 p \int d^4 q \frac{1}{P^2 P'^2 Q^2 Q'^2}. \quad (30)$$

The graphs are grouped into sets for which large cancellations of linear energy divergences occur. The notation, for example $1B(t, ij0)$ describes the fermion loop inserted on top of the original graph $1B$ connected with two transverse (indices i, j) and one Coulomb line to the rest of the graph. There are several original two-loop graphs (e.g. $1B, 2B, 3B$) which differ only in the positions of Coulomb and transverse lines. The momenta are defined as $p' = p - k$, $q' = q - k$, $r' = k - p - q$. We list the final results for the graphs.

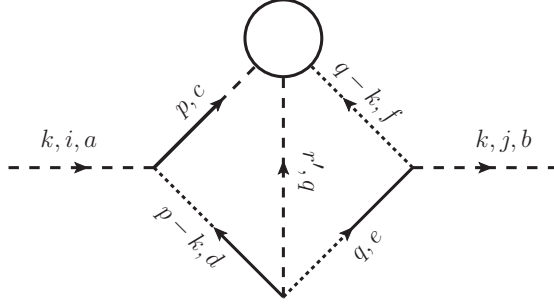


Figure 3: Graph $1B(t, ij0)$. There are two other graphs in which the pure Coulomb line is p' or q' rather than q' , giving $2B(t, ij0)$ and $3B(t, ij0)$ respectively. The arrow indicates the sense of momentum flow.

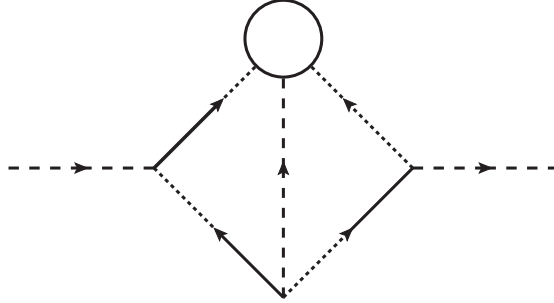


Figure 4: Graph $1B(t, 0j0)$. There are 3 other graphs obtained by moving the Coulomb line around the gluon loop.

4.1 Set 1

In this subsection we consider the graphs shown in fig.3 and fig.4, between which large cancellations of linear energy divergences take place.

The sum of 3 graphs (one representative graph is shown in fig.3) is

$$1B(t, ij0) + 2B(t, ij0) + 3B(t, ij0) = \alpha_{ab} P_i (Q + 2Q')_j \frac{1}{r_0'^2 p_0 q_0} [p_0^2 S(p) - r_0'^2 S(r')]. \quad (31)$$

We have 3 graphs obtained from graphs in (30) by rotating the internal lines about the vertical axis (keeping the external gluons fixed) giving

$$1B(t, 0jk) + 2B(t, 0jk) + 3B(t, 0jk) = \alpha_{ab} (2P + P')_i Q'_j \frac{1}{r_0'^2 p_0 q_0} [q_0^2 S(q') - r_0'^2 S(r')]. \quad (32)$$

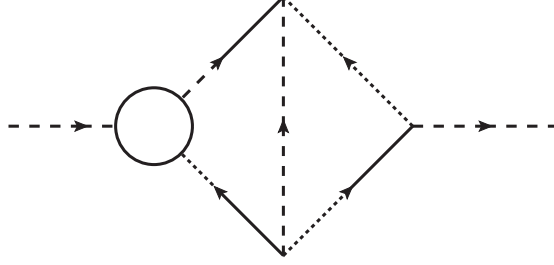


Figure 5: Graph $4B(l, ij0)$. There are two more distinct graphs in this class.

There are 4 graphs (the example $1B(t, 0j0)$ is shown in fig.4) where the fermion loop is connected to the rest of the graph with two Coulomb lines. Their sum amounts to

$$1B(t, 0j0) + 2B(t, 0j0) + 3B(t, 0j0) + 4B(t, 0j0) = -\alpha_{ab}(P_i Q_j + 2P_i Q'_j + P'_i Q'_j) \times \frac{1}{r_0'^2} \left\{ \frac{1}{q_0} [p_0 S(p) + r'_0 S(r')] + \frac{1}{p_0} [r'_0 S(r') + q'_0 S(q')] \right\}. \quad (33)$$

We see that individual terms in this set contain linear energy divergences, for example $\frac{1}{r_0'^2}$. But in the sum of eqs.(31), (32) and (33) large cancellations of linear divergences occur, giving for the first set

$$Set1 = -\alpha_{ab} \left\{ \frac{1}{r_0'^2} \left[\frac{q'_0}{p_0} P_i Q_j S(q') + \frac{p_0}{q_0} P'_i Q'_j S(p) \right] + \frac{2}{p_0 q_0} P_i Q'_j S(r') \right\}. \quad (34)$$

4.2 Set 2

In this set we treat graphs with fermion loop on the left side, connected to the incoming gluon. There are 3 distinct graphs like the graph $4B(l, ij0)$ shown in Fig.5. Their sum is

$$4B(l, ij0) + 5B(l, ij0) + 6B(l, ij0) = -\alpha_{ab} P_i (Q + 2Q')_j \frac{1}{r_0'^2} S(p). \quad (35)$$

We have two graphs where the fermion loop connects through two Coulomb lines.

$$1B(l, 0i0) = \alpha_{ab} \frac{1}{r_0'^2} Q'_j [P_i S(p) + P'_i S(p')], \quad (36)$$

$$1B'(l, 0i0) = \alpha_{ab} \frac{1}{r_0'^2} Q_j [P_i S(p) + P'_i S(p')]. \quad (37)$$

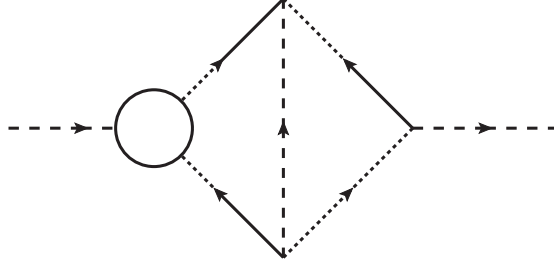


Figure 6: Graph $1B(l, 0i0)$. The other graph $1B'(l, 0i0)$ has p and q lines interchanged.

In the $S(p')$ terms in (36) and (37) we make the change of variables of integration $p \leftrightarrow -p', q \leftrightarrow -q', r \leftrightarrow -r, k \leftrightarrow k, (i, j \leftrightarrow i, j)$ and obtain

$$1B(l, 0i0) + 1B'(l, 0i0) = \alpha_{ab} \frac{1}{r_0^2} (Q + Q')_j \times 2P_i S(p). \quad (38)$$

Again large cancellations of linear divergences occur in the sum of (38) and (35) giving

$$Set2 = \alpha_{ab} \frac{1}{r_0^2} P_i Q_j S(p). \quad (39)$$

4.3 Set 3

Set3 consists of 5 graphs which are rotations about the vertical axis (keeping the external gluons fixed) of the graphs contained in *Set2*.

$$Set3 = \alpha_{ab} \frac{1}{r_0^2} P'_i Q'_j S(q'). \quad (40)$$

In the limit of large linear divergences (i.e. $r'_0 = -p_0 - q'_0 \approx 0$) the sum of the first three sets of diagrams gives

$$Set1 + Set2 + Set3 = \alpha_{ab} \left\{ \frac{1}{r_0^2} (P_i Q_j + P'_i Q'_j) [S(p) + S(q')] - \frac{2}{p_0 q'_0} P_i Q'_j S(r') \right\}. \quad (41)$$

4.4 Set 4

This set contains four self-energy graphs. Their sum cancels the linear divergence in (41).

$$Set4 = -\alpha_{ab} \frac{1}{r_0^2} (P_i Q_j + P'_i Q'_j) [S(p) + S(q')] \quad (42)$$

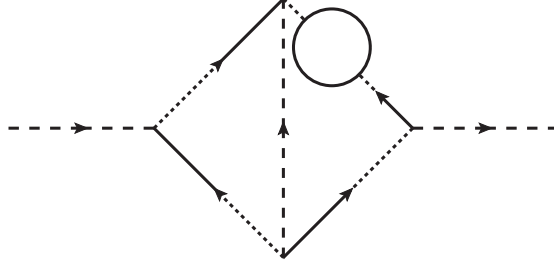


Figure 7: Graph $SE1$ which represents the four graphs in $Set4$. We insert the fermion loop on q' or p line. All other graphs which could be drawn in this set are rotations about the horizontal axis and so identical to the first four graphs.

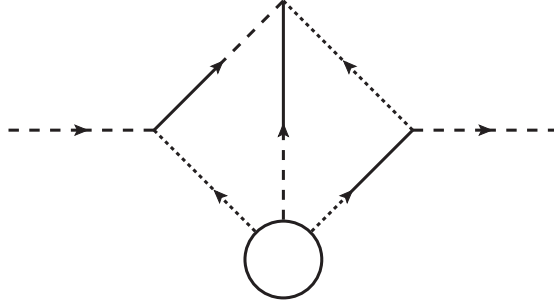


Figure 8: Graph $1B(b, 0i0)$. The fermion loop on bottom is connected with two Coulomb lines to the rest of the graph.

4.5 Set 5

There are four graphs in this set. We give the results and respective figures.

$$1B(b, 0i0) = -\alpha_{ab} P_i Q_j \frac{1}{p_0 r'_0} \left\{ \frac{1}{p'_0} [q_0 S(q) + r'_0 S(r')] + \frac{1}{q_0} [p'_0 S(p') + r'_0 S(r')] \right\}, \quad (43)$$

$$1\tilde{B}(t, 0i0) = -\alpha_{ab} P_i Q_j \frac{1}{q_0 r'_0} \left\{ \frac{1}{q'_0} [p_0 S(p) + r'_0 S(r')] + \frac{1}{p_0} [q'_0 S(q') + r'_0 S(r')] \right\}, \quad (44)$$

$$1B(b, 0ij) = -\alpha_{ab} P_i Q_j \frac{1}{q_0 r'_0 p_0 p'_0} [r_0'^2 S(r') - q_0^2 S(q)], \quad (45)$$

$$1\tilde{B}(t, 0ij) = -\alpha_{ab} P_i Q_j \frac{1}{p_0 r'_0 q_0 q'_0} [r_0'^2 S(r') - p_0^2 S(p)]. \quad (46)$$

Again large cancellations of linear divergences occur in the sum of graphs in $Set5$ giving

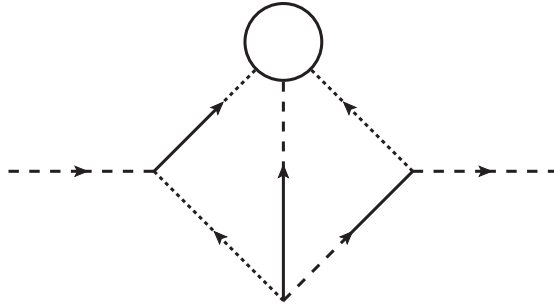


Figure 9: Graph $1\tilde{B}(t, 0i0)$

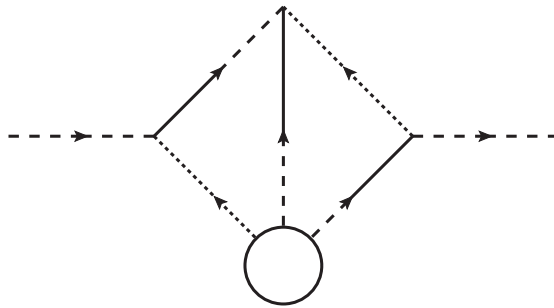


Figure 10: Graph $1B(b, 0ij)$

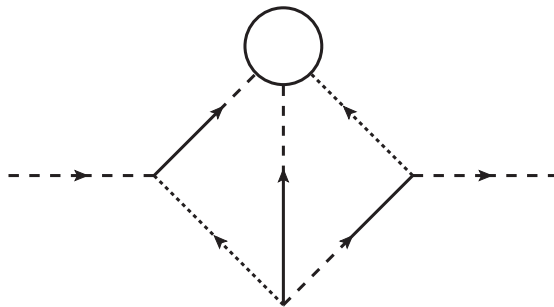


Figure 11: Graph $1\tilde{B}(t, 0ij)$

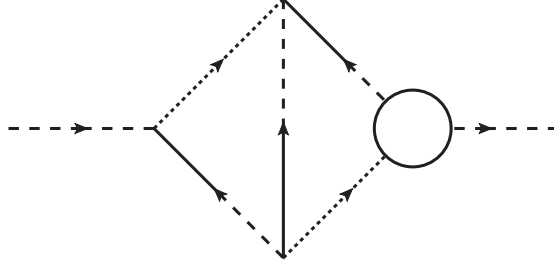


Figure 12: Graph $2B(r, 0ij)$

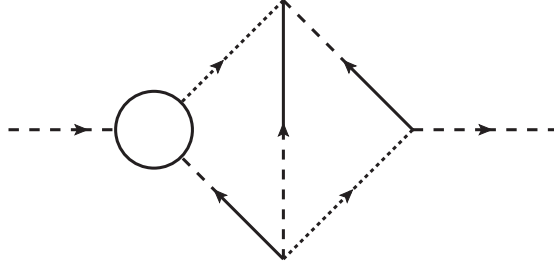


Figure 13: Graph $2\tilde{B}(l, 0ij)$

$$Set5 = -\alpha_{ab} \frac{1}{p_0 q_0 r'_0} [p_0'^2 S(p') + q_0' S(q')] \quad (47)$$

4.6 Set 6

There are only two graphs in this set.

$$2B(r, 0ij) = \alpha_{ab} P'_i Q'_j \frac{1}{p'_0 r'_0 q_0 q'_0} [k_0^2 S(k) - q_0'^2 S(q')]. \quad (48)$$

$$2\tilde{B}(l, 0ij) = \alpha_{ab} P'_i Q'_j \frac{1}{q'_0 r'_0 p_0 p'_0} [k_0^2 S(k) - p_0'^2 S(p')]. \quad (49)$$

In the high-energy limit we ignore terms $k_0 S(k)$ and take $\frac{q'_0}{q_0} \approx 1$, $\frac{p'_0}{p_0} \approx 1$, so the sum of two graphs in this set amounts to

$$Set6 = -\alpha_{ab} P'_i Q'_j \frac{1}{p'_0 q'_0 r'_0} [p'_0 S(p') + q'_0 S(q')]. \quad (50)$$

We also have a graph $1B(b, 00j)$ which has no K^2 contribution.

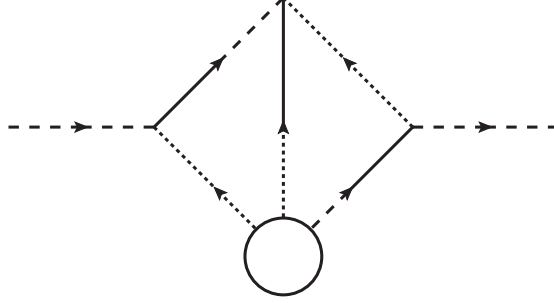


Figure 14: Graph $1B(b, 00j)$. This graph has no K^2 contribution.

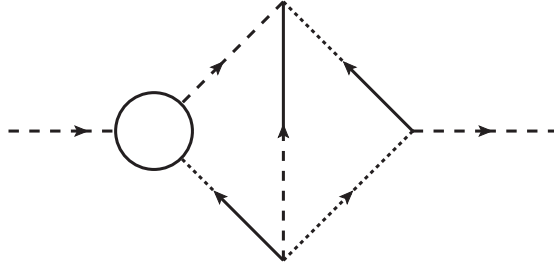


Figure 15: Graph $3B(l, ij0)$. There are two more distinct graphs with left insertion of the fermion loop.

4.7 Set 7

There are 3 graphs with a left vertex part insertion and 15 graphs with a self-energy insertion in this set.

The first three give

$$1B(l, ij0) + 2B(l, ij0) + 3B(l, ij0) = \alpha_{ab} P_i(Q + 2Q')_j \frac{1}{p_0 r'_0} S(p). \quad (51)$$

The graphs with self energy insertions give altogether

$$SE1B + SE2B + SE3B = -\alpha_{ab} P_i(Q + 2Q')_j \frac{1}{p_0 r'_0} [S(p) + S(p') + S(r') + S(q) + S(q')]. \quad (52)$$

The sum of (52) and (51) amounts to

$$Set7 = -\alpha_{ab} P_i(Q + 2Q')_j \frac{1}{p_0 r'_0} [S(p') + S(r') + S(q) + S(q')]. \quad (53)$$

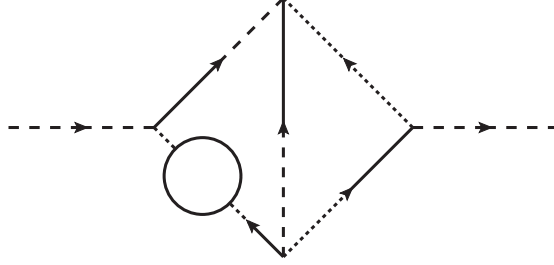


Figure 16: Graph $SE1B$. There are 15 graphs with self-energy insertions where the middle line is the $A_i E_j$ -transition. We draw just one representative of these graphs.

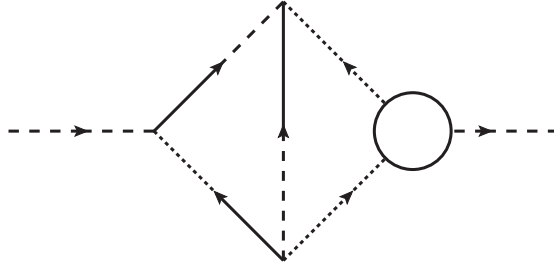


Figure 17: Graph $1\tilde{B}(r, 0i0)$

4.8 Set 8

Set8 consists of graphs which are rotations of graphs in *Set7* about the vertical axis and the change of variables of integration $p \leftrightarrow -p', q \leftrightarrow -q', k \leftrightarrow k, (i, j \leftrightarrow i, j)$

$$Set8 = -\alpha_{ab}(P + 2P')_i Q_j \frac{1}{q_0 r'_0} [S(q') + S(r') + S(p) + S(p')]. \quad (54)$$

4.9 Set 9

There are two graphs in this set.

$$1\tilde{B}(r, 0i0) = \alpha_{ab} \frac{1}{p_0 r'_0} P_i [Q_j S(q) + Q'_j S(q')]. \quad (55)$$

$$1\tilde{B}(l, 0i0) = \alpha_{ab} \frac{1}{q_0 r'_0} Q_j [P_i S(p) + P'_i S(p')]. \quad (56)$$

The sum of these two graphs is

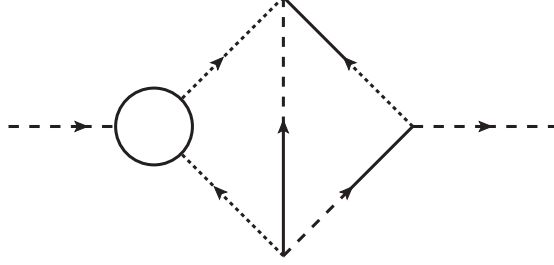


Figure 18: Graph $1\tilde{B}(l, 0i0)$

$$Set9 = \alpha_{ab} \left\{ \frac{1}{p_0 r'_0} P_i [Q_j S(q) + Q'_j S(q')] + \frac{1}{q_0 r'_0} Q_j [P_i S(p) + P'_i S(p')] \right\}. \quad (57)$$

4.10 Set 10

We have cancelled linear energy divergences in the first nine sets of graphs. Using changes of variables of integration $p \leftrightarrow -p', q \leftrightarrow -q', r \leftrightarrow -r, k \leftrightarrow k, (i, j) \leftrightarrow (i, j)$ and $\frac{p'_i}{p_0} \approx 1, \frac{q'_j}{q_0} \approx 1$, we transform $S(p)$ and $S(q)$ terms into $S(p')$ and $S(q')$ and obtain for the sum of the graphs so far

$$\begin{aligned} & Set1 + Set2 + \dots + Set9 \\ = & -\alpha_{ab} \left\{ S(r') \left[\frac{1}{p_0 q'_0} P_i Q'_j + \frac{1}{p'_0 q_0} P'_i Q_j + \frac{1}{p_0 r'_0} P_i (Q + 2Q')_j + \frac{1}{q_0 r'_0} (P + 2P')_i Q_j \right] \right. \\ & \left. + S(p') \left[\frac{1}{q_0 r'_0} (P + P')_i Q_j + \frac{1}{q'_0 r'_0} P'_i Q'_j \right] + S(q') \left[\frac{1}{p_0 r'_0} P_i (Q + Q')_j + \frac{1}{p'_0 r'_0} P'_i Q'_j \right] \right\}. \quad (58) \end{aligned}$$

But we have two more V -graphs (graphs with fermion loop three-point function) which contain linear energy divergences. They are

$$2B(b, 0i0) = -\alpha_{ab} P_i Q'_j \left\{ \frac{1}{p_0 p'_0} [S(r') - S(q)] + \frac{1}{p_0 q_0} [S(r') - S(p')] - \frac{1}{p_0 r'_0} [S(q) + S(p')] \right\} \quad (59)$$

and

$$2\tilde{B}(t, 0i0) = -\alpha_{ab} P'_i Q_j \left\{ \frac{1}{q_0 q'_0} [S(r') - S(p)] + \frac{1}{q_0 p_0} [S(r') - S(q')] - \frac{1}{q_0 r'_0} [S(p) + S(q')] \right\}. \quad (60)$$

Thus the total contribution from vertex part and self-energy insertions is given by the sum of (58), (59) and (60).

The graph where the fermion loop is connected to the rest of the graph with three Coulomb lines (function V_{000}) has no K^2 contribution.

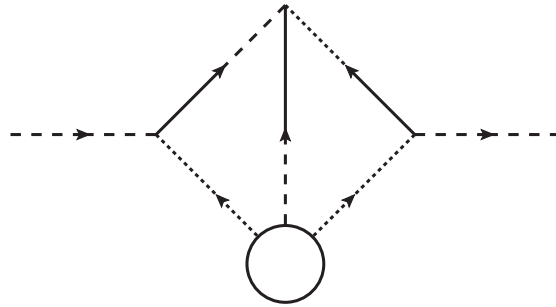


Figure 19: Graph $2B(b, 0i0)$

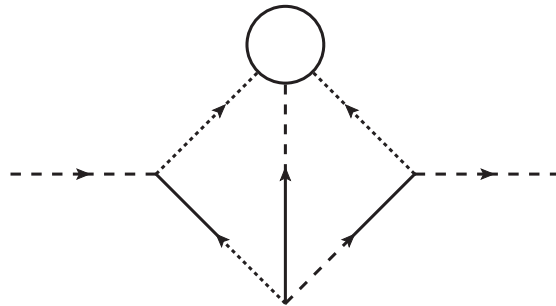


Figure 20: Graph $2\tilde{B}(t, 0i0)$

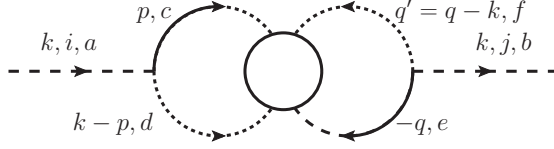


Figure 21: Graph W1. Fermion loop insertion is connected with three Coulomb and one transverse line to the rest of the graph.

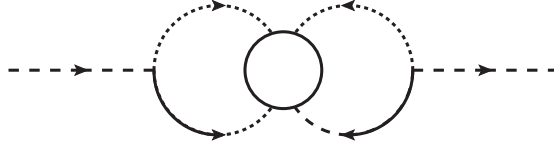


Figure 22: Graph W2

4.11 W GRAPHS

W -graphs contain 4-point fermion loop insertion. We start with the sum of two graphs with the W_{000l} function.

$$W1 + W2 = -\alpha_{ab}(P + P')_i Q_j \left\{ \frac{1}{p_0 p'_0} [S(q') - S(r')] + \frac{1}{q_0 q'_0} [S(p) - S(r')] + \frac{1}{p'_0 q'_0} [S(q) - S(r')] \right. \\ \left. - \frac{1}{q_0 p'_0} S(r') + \frac{1}{q_0 (q' + p)_0} [S(p') - S(q)] + \frac{1}{q_0 p'_0 k_0} [q_0 S(q) - q'_0 S(q')] \right\}. \quad (61)$$

Next two graphs are obtained from $W1$ and $W2$ by rotating them about the vertical axis and the change of variables of integration $p \leftrightarrow -p', q \leftrightarrow -q', k \leftrightarrow k, (i, j \leftrightarrow i, j)$ (so we do not draw them explicitly).

$$\widetilde{W}1 + \widetilde{W}2 = -\alpha_{ab} P'_i (Q + Q')_j \left\{ \frac{1}{q_0 q'_0} [S(p) - S(r')] + \frac{1}{p_0 p'_0} [S(q') - S(r')] + \frac{1}{q_0 p_0} [S(p') - S(r')] \right. \\ \left. - \frac{1}{p'_0 q_0} S(r') + \frac{1}{p'_0 (p + q')_0} [S(q) - S(p')] + \frac{1}{p'_0 q_0 k_0} [p_0 S(p) - p'_0 S(p')] \right\} \quad (62)$$

Two following graphs contain fermion loop insertion connected to the rest of the graph with two Coulomb and two transverse lines.

$$W3 = \alpha_{ab} P_i Q_j \left\{ \frac{1}{p_0 p'_0} [S(q) - S(r')] + \frac{1}{q_0 q'_0} [S(p) - S(r')] - \frac{2}{p_0 q_0} S(r') \right\} \quad (63)$$

$$W4(K^2) = 0 \quad (64)$$

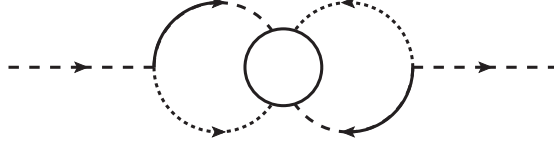


Figure 23: Graph $W3$

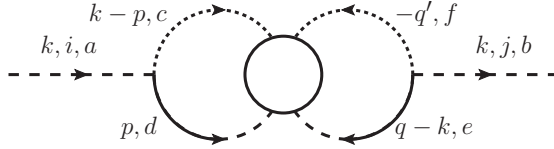


Figure 24: Graph $W4$. This graph has no K^2 contribution.

Equations (61) and (62) show new type of quadratic divergence in the form $\frac{1}{k_0}$. These divergences will be cancelled by graphs which contain W_{0000} insertion. There are two such distinct graphs. We list the sum of their contribution.

$$\begin{aligned}
 W_{0000}^1 + W_{0000}^2 = & -\frac{1}{2} \alpha_{ab} (P + P')_i (Q + Q')_j \left\{ \frac{1}{p_0 q_0} [S(k) + S(r') - S(q') - S(p')] \right. \\
 & - \frac{1}{p'_0 q'_0} [S(k) + S(r') - S(p) - S(q)] + \left[\frac{1}{q_0 q'_0} S(r') + \frac{1}{q_0 k_0} S(p') - \frac{1}{q'_0 k_0} S(p) \right] \\
 & \left. + \left[\frac{1}{p_0 p'_0} S(r') + \frac{1}{p_0 k_0} S(q') - \frac{1}{p'_0 k_0} S(q) \right] \right\} \quad (65)
 \end{aligned}$$

The tricky terms with $\frac{1}{k_0}$ in (65) we denote as

$$\begin{aligned}
 X_p &= \frac{1}{q_0 k_0} S(p') - \frac{1}{q'_0 k_0} S(p), \\
 X_q &= \frac{1}{p_0 k_0} S(q') - \frac{1}{p'_0 k_0} S(q). \quad (66)
 \end{aligned}$$

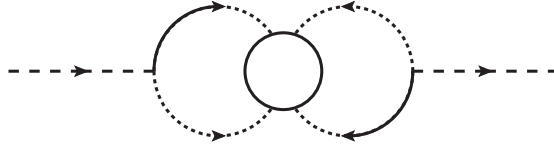


Figure 25: Graph W_{0000}^1 . Four Coulomb lines attach to the fermion loop. The graph contains divergences of the form $\frac{1}{k_0}$.

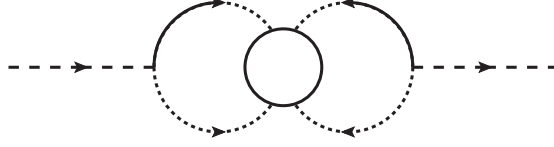


Figure 26: Graph W_{0000}^2 . The graph shows divergences of the form $\frac{1}{k_0}$.

Then each of X_p and X_q is invariant under $p, q \rightarrow -p', -q'$. Therefore, by making these changes of variables, we have

$$-\frac{1}{2}\alpha_{ab}(P+P')_i(Q+Q')_j[X_p+X_q] = -\alpha_{ab}P'_i(Q+Q')_jX_p - \alpha_{ab}(P+P')_iQ_jX_q. \quad (67)$$

First we prove the cancellation of the tricky $\frac{1}{k_0}$ divergences. Such terms exist in (61), (62) and (67). The sum of the last terms in (61) and (62) with (67) is

$$\begin{aligned} & -\alpha_{ab}(P+P')_iQ_j\left\{\frac{1}{p'_0k_0}[S(q)-S(q')] + \frac{1}{q_0p'_0}S(q') + \frac{1}{p_0k_0}S(q') - \frac{1}{p'_0k_0}S(q)\right\} \\ & -\alpha_{ab}P'_i(Q+Q')_j\left\{\frac{1}{q_0k_0}[S(p)-S(p')] + \frac{1}{p'_0q_0}S(p) + \frac{1}{q_0k_0}S(p') - \frac{1}{q'_0k_0}S(p)\right\} \\ = & \alpha_{ab}(P+P')_iQ_j\left\{\frac{1}{p_0p'_0}S(q') - \frac{1}{q_0p'_0}S(q')\right\} + \alpha_{ab}P'_i(Q+Q')_j\left\{\frac{1}{q_0q'_0}S(p) - \frac{1}{p'_0q_0}S(p)\right\} \end{aligned} \quad (68)$$

The important point to notice is that after cancellation of $\frac{1}{k_0}$ divergences, we are left with linear energy divergences in (68). Now we are ready to prove the cancellation of linear divergences. Linear divergences (i.e. terms with $\frac{1}{p_0p'_0}$ and $\frac{1}{q_0q'_0}$) are parts of (65), (61), (62), (63), (59) and (60).

From (65) taking into account (68) we have

$$\begin{aligned} A_{ij}^{ab} = & -\frac{1}{2}\alpha_{ab}(P+P')_i(Q+Q')_j\left[\frac{1}{q_0q'_0}S(r') + \frac{1}{p_0p'_0}S(r')\right] \\ & +\alpha_{ab}\left[(P+P')_iQ_j\frac{1}{p_0p'_0}S(q') + P'_i(Q+Q')_j\frac{1}{q_0q'_0}S(p)\right] \\ = & \alpha_{ab}\left\{(P+P')_iQ_j\frac{1}{p_0p'_0}[S(q')-S(r')] + P'_i(Q+Q')_j\frac{1}{q_0q'_0}[S(p)-S(r')]\right\} \end{aligned} \quad (69)$$

The linearly divergent part of (61) is

$$B_{ij}^{ab} = -\alpha_{ab}(P+P')_iQ_j\left\{\frac{1}{p_0p'_0}[S(q')-S(r')] + \frac{1}{q_0q'_0}[S(p)-S(r')]\right\} \quad (70)$$

In (62) the linearly divergent part is

$$C_{ij}^{ab} = -\alpha_{ab}P'_i(Q+Q')_j\left\{\frac{1}{p_0p'_0}[S(q')-S(r')] + \frac{1}{q_0q'_0}[S(p)-S(r')]\right\} \quad (71)$$

From W3 in (63),

$$D_{ij}^{ab} = \alpha_{ab} P_i Q_j \left\{ \frac{1}{p_0 p'_0} [S(q) - S(r')] + \frac{1}{q_0 q'_0} [S(p) - S(r')] \right\}. \quad (72)$$

Graph $2B(b, 0i0)$ in (59) contributes

$$E_{ij}^{ab} = -\alpha_{ab} P_i Q'_j \frac{1}{p_0 p'_0} [S(r') - S(q)] \quad (73)$$

and graph $2\tilde{B}(t, 0i0)$ in (60) gives

$$F_{ij}^{ab} = -\alpha_{ab} P'_i Q_j \frac{1}{q_0 q'_0} [S(r') - S(p)]. \quad (74)$$

It is easy to check that the sum of equations (69) to (74) gives zero (using the symmetry $p \rightarrow -p', q \rightarrow -q', (i, j) \rightarrow (i, j)$).

4.12 *A-divergences*

Having verified that all the linear energy divergences cancel, we are ready to come to the main point of the paper, the cancellation or otherwise of the *A-ambiguous* integrals like (3). We collect the remaining *A-divergences*. From (65) we have,

$$\begin{aligned} \tilde{A}_{ij}^{ab} &= -\frac{1}{2} \alpha_{ab} (P + P')_i (Q + Q')_j \left\{ \frac{1}{p_0 q_0} [S(r') - S(q') - S(p')] - \frac{1}{p'_0 q'_0} [S(r') - S(p) - S(q)] \right\} \\ &\quad - \alpha_{ab} \left\{ (P + P')_i Q_j \frac{1}{q_0 p'_0} S(q') + P'_i (Q + Q')_j \frac{1}{q_0 p'_0} S(p) \right\} \\ &= -\alpha_{ab} \frac{1}{q_0 p'_0} [(P + P')_i Q_j S(q') + P'_i (Q + Q')_j S(p)]. \quad (75) \end{aligned}$$

The remaining *A-divergences* in (61) are

$$\tilde{B}_{ij}^{ab} = -\alpha_{ab} (P + P')_i Q_j \left\{ \frac{1}{q'_0 p'_0} [S(q) - S(r')] - \frac{1}{p'_0 q_0} S(r') - \frac{1}{q_0 r'_0} [S(p') - S(q)] \right\}. \quad (76)$$

From (62) we have the *A-divergences*

$$\tilde{C}_{ij}^{ab} = -\alpha_{ab} P'_i (Q + Q')_j \left\{ \frac{1}{q_0 p_0} [S(p') - S(r')] - \frac{1}{p'_0 q_0} S(r') - \frac{1}{p'_0 r'_0} [S(q) - S(p')] \right\}. \quad (77)$$

The *A-divergence* in (63) is

$$\tilde{D}_{ij}^{ab} = -\alpha_{ab} \frac{2}{p_0 q_0} P_i Q_j S(r'). \quad (78)$$

In (59) we have

$$\tilde{E}_{ij}^{ab} = -\alpha_{ab} P_i Q'_j \left\{ \frac{1}{p_0 q_0} [S(r') - S(p')] - \frac{1}{p_0 r'_0} [S(q) + S(p')] \right\}. \quad (79)$$

In (60) the remaining divergence is

$$\tilde{F}_{ij}^{ab} = -\alpha_{ab} P'_i Q_j \left\{ \frac{1}{q_0 p_0} [S(r') - S(q')] - \frac{1}{q_0 r'_0} [S(p) + S(q')] \right\} \quad (80)$$

Summing up (75) to (80) with (58) (using the same changes of variables to transform $S(p)$ and $S(q)$ terms into $S(p')$ and $S(q')$) and the rule of factorization (5), the final result for the sum of all the A -divergences is

$$\begin{aligned} X_{ij}^{ab} = \alpha_{ab} \{ & S(r') [P_i Q_j \left(\frac{1}{p'_0 q_0} + \frac{1}{p_0 q'_0} + \frac{1}{p_0 q_0} \right) + \frac{2}{p_0 q'_0} P_i Q'_j] \\ & - \frac{1}{p'_0 r'_0} P'_i Q_j S(p') - \frac{1}{q'_0 r'_0} P_i Q'_j S(q') \}. \end{aligned} \quad (81)$$

The A -divergences do not cancel out.

The first line of (81) contains terms like

$$\alpha_{ab} S(r') P_i Q_j \frac{1}{p_0 q'_0} \quad (82)$$

in which the μ^2 subtraction term in (10) gives zero contribution by the factorization rule (5). But the $(-r'^2)^{-\epsilon}$ term in (10) gives a non-zero contribution to (82) which is in fact proportional to $\Gamma(\frac{\epsilon}{2})$. The second line of (81), using a change of variables, and the identity

$$\frac{1}{p'_0 r'_0} + \frac{1}{q_0 r'_0} + \frac{1}{p'_0 q_0} = 0$$

(this identity is to be used only for large energies, it is consistent with (4) being convergent) and using the factorization rule, may be written

$$\alpha_{ab} P'_i Q_j \frac{1}{q_0 r'_0} [S(p') - S(q)]. \quad (83)$$

Again the μ^2 subtraction term in (10) cancels out, but the remaining two parts of (83) give different non-zero contributions, each proportional to $\Gamma(\frac{\epsilon}{2})$. Thus, in (81), the UV divergences and the A -integrals conspire to give a divergent result.

5 Conclusion

To two loop order, the non-convergent A -integrals of the form (3) are rendered harmless by the use of the identity (4). But to three loops, when there are

UV divergent sub-graphs, we find that a similar process fails to work. So we conclude that it is not possible to make sense of Coulomb gauge perturbation theory to three loop order.

Acknowledgements

This work was supported by the Ministry of Science and Technology of the Republic of Croatia under contract No. 098-0000000-2865(A.A.). We are grateful to Dr. G. Duplančić for drawing the figures.

References

- [1] A. Cucchieri, hep-lat/0612004, AIP Conf. Proc. **892**,22-28 (2007)
- [2] A. Andraši, J.C. Taylor, Eur. Phys. J. C **41**,377 (2005)
- [3] A. Andraši, J.C. Taylor, Ann. of Phys. **324**,No.10, 2179-2195 (2009)
- [4] R.N. Mohapatra, Phys. Rev. D4 **22**,378, 1007 (1971)
- [5] H. Cheng, E. C. Tsai, Phys. Lett. B **176** 130 (1986); Phys. Rev. Lett. **57** 511 (1986)
- [6] P. Doust, Ann. of Phys. **177**, 169 (1987)
- [7] N. Christ, T. D. Lee, Phys. Rev. D**22**, 939 (1980)
- [8] J. C. Taylor, in Physical and Nonstandard Gauges, Proceedings, Vienna, Austria 1989, edited by P. Gaigg, W. Kummer, M. Schweda